Institute for Advanced Technology
The University of Texas at Austin

U.S. ARMY

Validation of the Cavity Expansion Resistance Model for Ceramic Targets with Computer Simulations

Yehuda Partom
Institute for Advanced Technology
The University of Texas at Austin

and

David Littlefield
Southwest Research Institute

May 1993

IAT.R 0025

REPORT DOCUMENTATION PAGE

Form Approved
OMB NO. 0704-0188

1. AGENCY USE ONLY (Leave blank)	2. REPORT DATE	3. REPORT TYPE AND DATES COVERED
	May 1993	Technical Report

4. TITLE AND SUBTITLE

Validation of the Cavity Expansion Resistance Model for Ceramic Targets with Computer Simulations

5. FUNDING NUMBERS

Contract # DAAA21-90-D-0009

6. AUTHOR(S)

Y. Partom and D. Littlefield

7. PERFORMING ORGANIZATION NAME(S) AND ADDRESS(ES)

Institute for Advanced Technology
The University of Texas at Austin
4030-2 W. Braker Lane, #200
Austin, TX 78759

8. PERFORMING ORGANIZATION REPORT NUMBER

IAT.R 0025

9. SPONSORING / MONITORING AGENCY NAME(S) AND ADDRESS(ES)

U.S. Army Armament Research Development and Engineering Center
ATTN: SMCAR-IMI-I
Picainny Arsenal, NJ 07806-5000

10. SPONSORING / MONITORING AGENCY REPORT NUMBER

11. SUPPLEMENTARY NOTES

The view, opinions and/or findings contained in this report are those of the author(s) and should not be considered as an official Department of the Army position, policy, or decision, unless so designated by other documentation.

12a. DISTRIBUTION / AVAILABILITY STATEMENT

Approved for public release; distribution unlimited.

12b. DISTRIBUTION CODE

A

13. ABSTRACT *(Maximum 200 words)*

In previous work we developed a model to predict the resistance (R_t) of ceramic targets to long rod penetration. The model was based on the cavity expansion model of Bishop, Hill, and Mott. Here we use computer simulations with the CTH code to validate our R_t model. We show that our model reproduces quite well the increase of R_t with the strength-pressure parameter, and with the cap pressure in the strength model. The increase of R_t with impact velocity predicted by the model is somewhat higher than that obtained from the simulations. We propose an explanation for this discrepancy that needs to be verified.

14. SUBJECT TERMS

Cavity Expansion Model (CEM)
Ceramic Targets
CTH code

15. NUMBER OF PAGES

12

16. PRICE CODE

17. SECURITY CLASSIFICATION OF REPORT	18. SECURITY CLASSIFICATION OF THIS PAGE	19. SECURITY CLASSIFICATION OF ABSTRACT	20. LIMITATION OF ABSTRACT
Unclassified	Unclassified	Unclassified	UL

Validation of the Cavity Expansion Resistance Model for Ceramic Targets with Computer Simulations

Yehuda Partom
Institute for Advanced Technology
The University of Texas at Austin

and

David Littlefield
Southwest Research Institute

Abstract—In reference 1 we developed a model to predict the resistance (R_t) of ceramic targets to long rod penetration. The model is based on the cavity expansion model of Bishop, Hill, and Mott. Here we use computer simulations with the CTH code to validate our R_t model. We show that our model reproduces quite well the increase of R_t with the strength-pressure parameter, and with the cap pressure in the strength model. The increase of R_t with impact velocity predicted by the model is somewhat higher than that obtained from the simulations. We propose an explanation for this discrepancy that needs to be verified.

Introduction

In reference 1 we develop a model to predict the resistance (R_t, as defined in Tate's[2] penetration model) of ceramic targets to long rod penetration. The model is based on the cavity expansion model (CEM) of Bishop, Hill and Mott.[3] In reference 1, we assume that the strength of brittle materials (ceramics) can be represented by the material model shown in Figure 1 (taken from reference 1). The upper curve represents the fracture condition. When the state point (Y, P—where Y is the equivalent shear stress and P is the pressure) reaches the fracture curve, the material fractures (becomes granular) and is able to flow. The lower curve represents the flow stress condition. When the material is fractured and can flow its state point can be either below the curve (elastic response) or on it (plastic flow). The essential features of this strength model are the dependence of flow stress on pressure (known as the Mohr-Coulomb response for granular materials), and the strength drop upon fracture.

In reference 1, we apply this strength model to the CEM and obtain expressions for R_t. The main outcome is that R_t increases with projectile velocity (V), which results from the pressure dependence of the flow stress. As stated in reference 1, the model needs validation, and maybe even some calibration. The crucial assumptions in the model that need validation are:

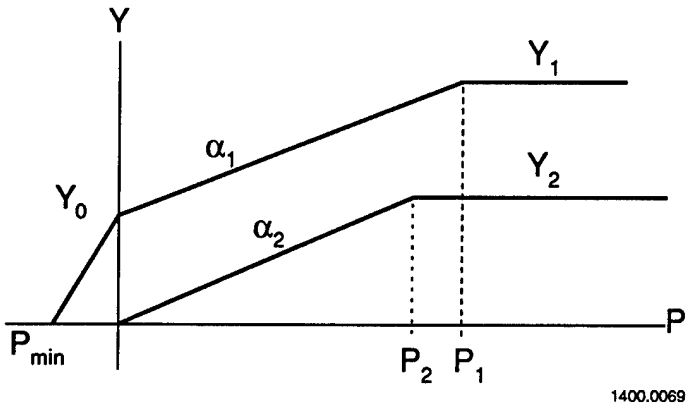

Figure 1. **Schematic strength model for ceramics.**

— The cylindrical CEM (which is a quasi-static model) can be applied to long rod penetration (which is a high rate dynamic process).

— The pressure field around the opening cavity is approximately homogeneous and can be represented by $P_d = \frac{1}{2}\rho_t u^2$, where ρ_t is the target density and u the penetration velocity.

In our view, the best way to validate the resistance model is by computer simulations. Comparing to experiments, we can never know what causes disagreements. They can be due to an inadequate material model or to the R_t model, or both. Comparing to simulations, in which we use the same material model, any disagreement is due to the R_t model.

We ran six simulations with the CTH code.[4] The parameters changed were: impact velocity v (1.5 and 2.5 Km/s), the slopes $\alpha_1 = \alpha_2$ (0.5 and 1), and the cap pressure $P_1 = P_2$ (10 and 4 GPa). From the results we extract R_t values and compare to the model predictions. Agreement is reasonable.

In what follows, we first describe the simulations and the results obtained from them. We then compare the simulation results to model predictions, discuss the overall agreement, and indicate possible reasons for disagreement.

Simulations

Simulations were performed at SwRI with the CTH code.[4] The projectile is a L/D = 10 tungsten alloy rod with D = 7.87 mm. The target has a depth of 254 mm and a diameter of 222 mm. In the projectile and in the target where most of the "action" takes place the cell size is 0.787 x 0.787 mm. Beyond that the target cells grow gradually by a factor of 1.022 in the radial direction and 1.018 in the longitudinal direction. The lateral

and back boundaries of the target were free boundaries. Since no detectable deformation occurred in any of the runs at either boundary, we concluded that these boundaries were virtually semi-infinite and had no effect on the penetration process. We also repeated one of the runs with a transmitting lateral boundary and got essentially the same result.

Equations of state for the projectile and target materials are those used routinely at SwRI for these materials. (Our R_t model and the Tate penetration model do not depend on equations of state.) The density of the projectile was 17.3 g/cc. The flow stress of the projectile was represented by the viscoplastic model routinely used at SwRI for tungsten alloys. It has been concluded from many previous simulations that this viscoplastic model represents a dynamic flow stress of $Y_P = 2.0$ GPa. The density and shear modulus of the target material (99.5 alumina) were : $\rho_t = 3.96$ g/cc, $G = 152$ GPa. The strength model parameters used for the target were:

$Y_o = 1.5$ GPa
$\alpha_1 = \alpha_2 = 0.5, 1.0$
$P_1 = P_2 = 10.0, 4.0$GPa
$P_{min} = -0.5$ GPa

There were six runs as follows:

Table 1
Varying Parameters in the Six Simulation Runs

Number	V Km/S	α_1, α_2	P_1, P_2 GPa
1	1.5	0.5	10.0
2	2.5	0.5	10.0
3	1.5	1.0	10.0
4	2.5	1.0	10.0
5	1.5	1.0	4.0
6	2.5	1.0	4.0

We present the results of these runs by means of penetration curves (p versus L, where p is the current penetration and L the current projectile length). They are shown in Figures 2.1 to 2.6. Penetration curves include all the information needed to extract R_t values. The usual way to fit an R_t value is by running a Tate code and adjusting R_t until the final penetration depth is matched. We refer to R_t obtained in this way as "effective R_t" and denote it by $\overline{R}_t$. Another way is to extract R_t from the slope of the penetration curve (s) where:

$$s = -\frac{dp}{dL} = -\frac{dp/dt}{dL/dt} = \frac{u}{v-u} \quad . \tag{1}$$

By substituting u in terms of s and v into Tate's equation it follows that:

$$R_t - Yp = \tfrac{1}{2}\rho_p v^2 f(s) \quad , \tag{2}$$

where:

$$f(s) = \frac{1 - \left(\frac{s}{s_h}\right)^2}{(1+s)^2} \quad , \tag{3}$$

and $s_h = (\rho_p/\rho_t)^{1/2}$ is the so called hydrodynamic limit. In Figures 2.1 to 2.6 we show where the slopes s are taken and the values obtained.

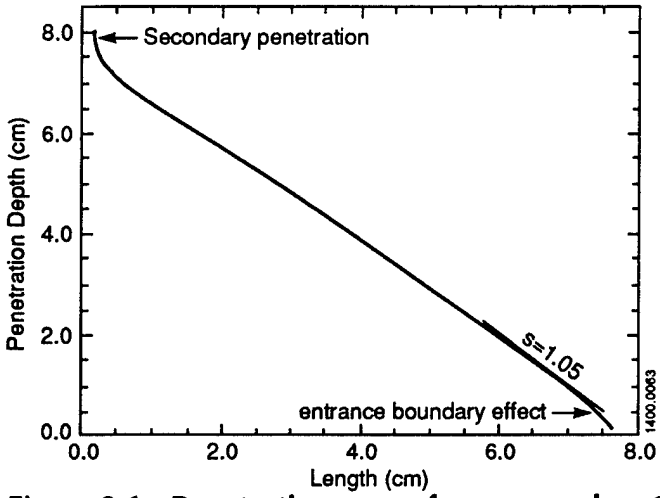

Figure 2.1. **Penetration curve for run number 1.**

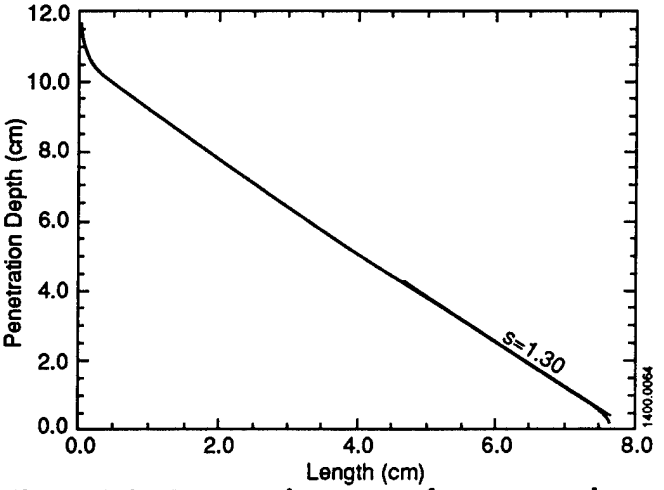

Figure 2.2. **Penetration curve for run number 2.**

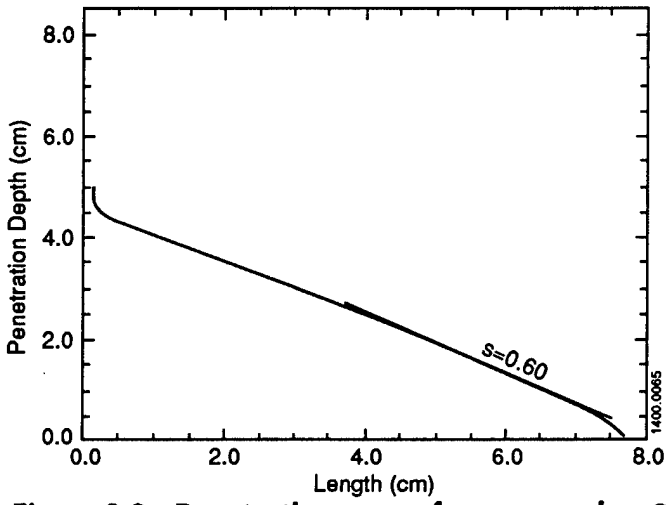

Figure 2.3. **Penetration curve for run number 3.**

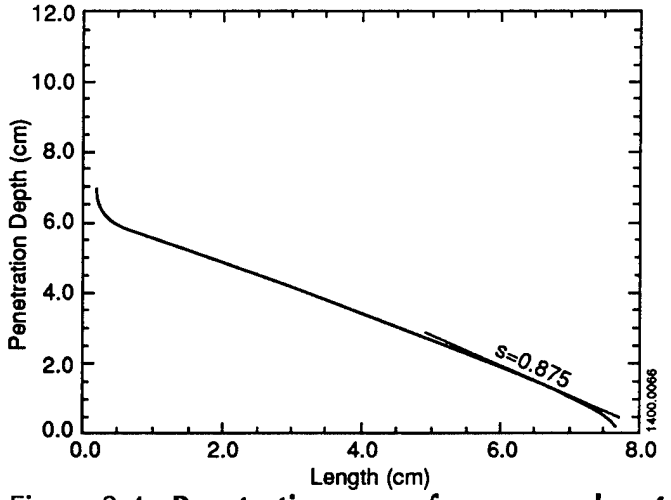

Figure 2.4. **Penetration curve for run number 4.**

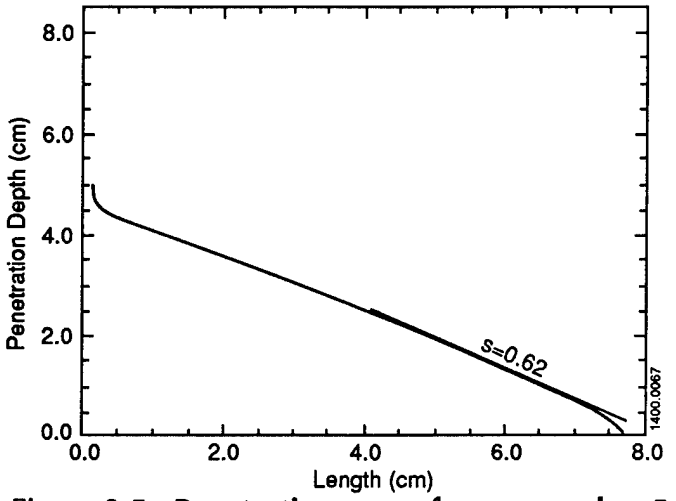

Figure 2.5. **Penetration curve for run number 5.**

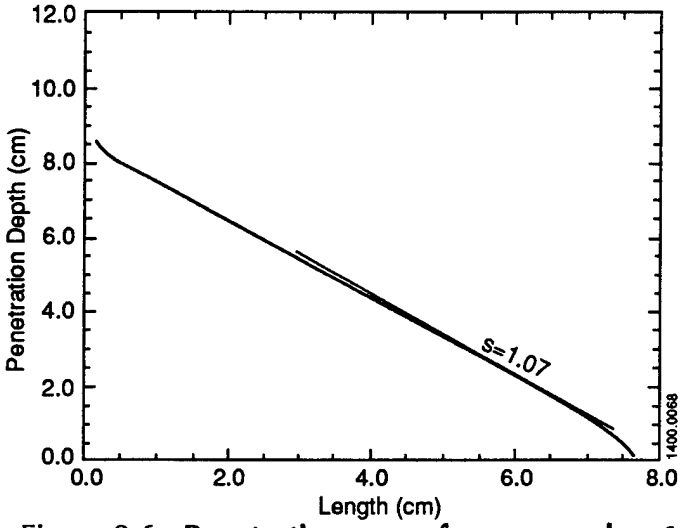

Figure 2.6. **Penetration curve for run number 6.**

We extracted $\overline{R}_t$ values only for Cases 1 and 2 (Table 1). The final penetrations (p_f) and values obtained are given in Table 2.

Table 2
Final Penetrations and $\overline{R}_t$ Values for Cases 1 and 2

Number	p_f (mm)	$\overline{R}_t$ (GPa)
1	80.8	4.63
2	116.2	5.76

It should be noted that the computations were stopped when the pressure dropped to zero. This means that the actual penetrations are even somewhat larger than these p_f values (and the $\overline{R}_t$ derived somewhat smaller). We show later that $\overline{R}_t$ values are too low compared to the resistance model predictions and that the model predictions should be compared to R_t values extracted from the slopes s. Using the slopes s shown in Figures 2.1 to 2.6 we obtain by equations 2 and 3 resistance values (R_t) for Cases 1 to 6 as given in Table 3.

Table 3
Extraction of R_t Values from Simulation Results

Number	s	f(s)	R_t-Y_p (GPa)	R_t (GPa)
1	1.05	0.179	3.48	5.48
2	1.30	0.117	6.33	8.33
3	0.60	0.359	6.99	8.99
4	0.875	0.235	12.70	14.70
5	0.62	0.348	6.77	8.77
6	1.07	0.174	9.39	11.39

It is evident that R_t increases with impact velocity. In the next section we present the resistance model predictions for the same material parameters and compare to resistance values extracted from the simulations.

Resistance Model Predictions Compared to Simulation Results

We evaluated the resistance model expressions derived in reference 1 as a function of impact velocity v for the following parameters:

ρ_p = 17.3 g/cc, Y_p = 2. GPa, ρ_t = 3.89 g/cc, G = 152 GPa, Y_o = 1.5 GPa, and α_1, α_2, P_1 and P_2 as in Table 1. (We inadvertently used ρ_t = 3.89 instead of 3.96 g/cc, but in view of the minor effect on the results, less than .5% in R_t, we did not repeat the computations.)

To have a measure for differences between model predictions and simulation results we introduce the factor k in the dynamic pressure definition, namely:

$P_d = \frac{1}{2} k \rho_t u^2$ (in reference 1 we used k = 1). (4)

In Figure 3 we show model predictions of R_t (V) curves for Cases 1, 2 ($\alpha_1 = \alpha_2 =$ 0.5, $P_1 = P_2$ = 10 GPa) for different values of k.

The two circles (o) are the $\overline{R}_t$ values from Table 2. The two plus (+) signs are the R_t values for Cases 1, and 2 in Table 3. We see that the $\overline{R}_t$ values are quite low. This is because they contain the low resistance near the entrance boundary and the very low, or even zero resistance during the secondary penetration phase (see Figure 2.1). The R_t values compare more reasonably with the model predictions. We get k = 0.9 and 0.6 for V = 1.5 and 2.5 Km/s, respectively. Later on we try to explain why k for V = 2.5 Km/s is lower than k for V = 1.5 Km/s. In Figure 4 we show R_t results for Cases 1 and 2 (lower curves) and for Cases 3 and 4 (upper curves). We see that the influence of the slopes in the strength model (α_1, α_2) is reproduced reasonably well.

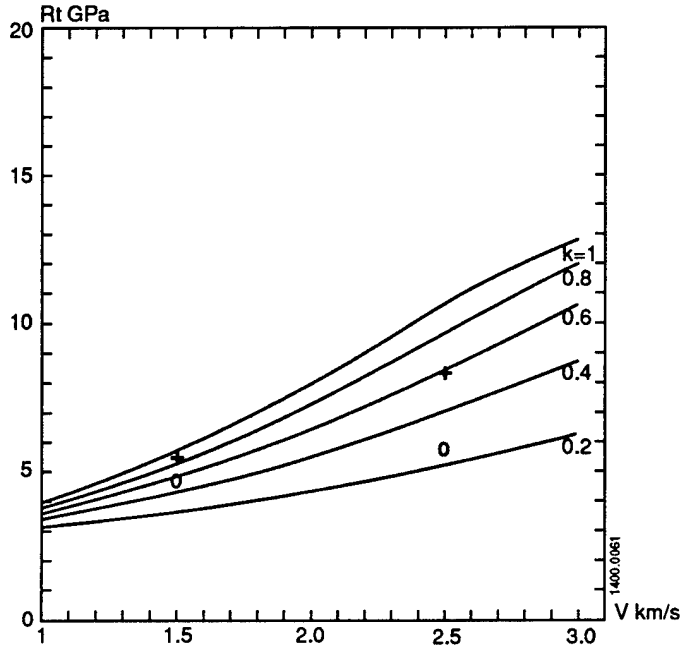

Figure 3. **Comparison of model predictions to simulation results for Cases 1 and 2; o are $\overline{R_t}$ values from Table 2. Plus signs (+) are R_t values from Table 3.**

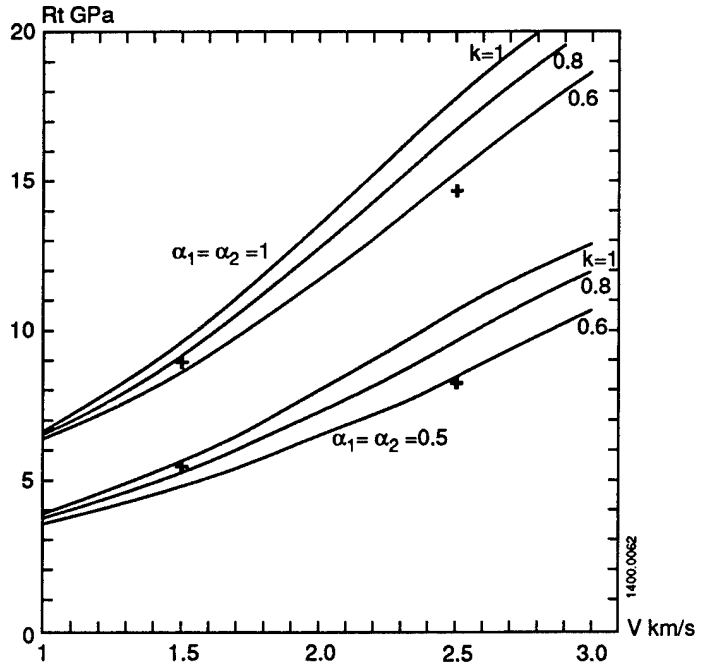

Figure 4. **Comparison of model predictions to simulation results. Lower curves for Cases 1 and 2. Upper curves for Cases 3 and 4. Plus signs (+) from Table 3.**

In Figure 5 we show R_t results for Cases 3 and 4 (upper curves) and for Cases 5 and 6 (lower curves). We see that the influence of the cap pressure (P_1, P_2) is reproduced reasonably well.

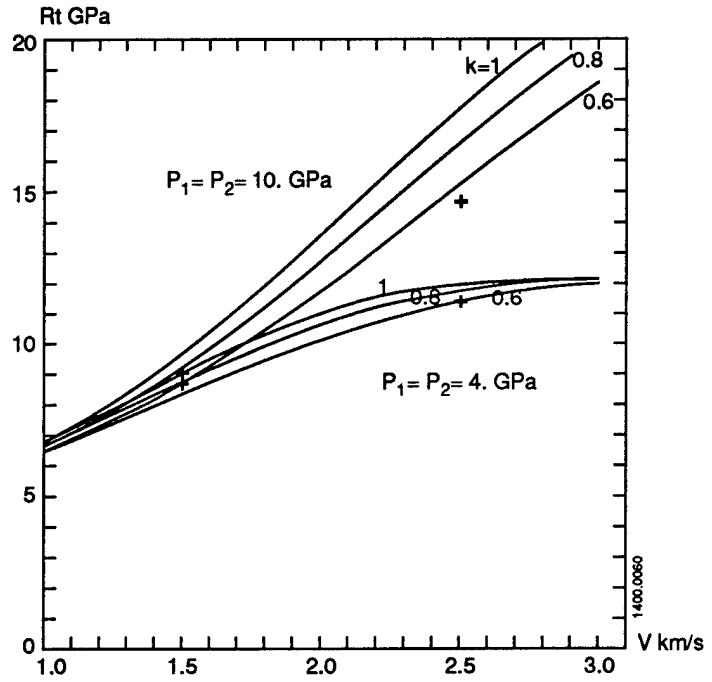

Figure 5. **Comparison of model predictions to simulation results. Upper curves for Cases 3 and 4. Lower curves for Cases 5 and 6. Plus signs (+) from Table 3.**

For all cases, the 2.5 Km/s simulation results correspond to a lower k value than that for 1.5 Km/s. One possible reason for that is the apparent decrease in resistance caused by the increase in the radial flow field at the front of the penetrating projectile head at higher velocity. Anderson, et al.[5] pointed out this effect for RHA steel. There is no reason why it should not exist for ceramic targets as well. But as R_t for ceramics increases with velocity, the radial flow effect is only able to diminish this increase. Another possible reason has to do with the radial decrease of pressure. In the model we don't include this decrease, and its influence is represented by k in equation 4. We also note that the flow field is more localized at high velocity. This can be seen in Table 4, where we show the distance at which the axial velocity falls to a fraction of its peak value, normalized by the extent of the plastic zone. The value is higher at higher velocity. The localization of the flow field apparently results in a lower penetration resistance.

Table 4
Scaled Distances (Relative to Plastic Zone Extent)
for 50% and 75% Axial Velocity Decrease for Runs 1 and 2

V (Km/s)	t (μs)	$\frac{\Delta x\ 50\%}{\Delta x \text{ pl. zone}}$	$\frac{\Delta x\ 75\%}{\Delta x \text{ pl. zone}}$
1.5	20	.082	.124
	60	.090	.161
	100	.076	.168
2.5	10	.072	.130
	30	.054	.103
	50	.051	.108
	70	.050	.107

Conclusions

In reference 1, we developed a model to predict the resistance (R_t) of brittle materials to long rod penetration. Assuming that the strength of brittle materials increases with pressure the model predicts that R_t increases with impact velocity.

Here we validate the predictions of our model by comparing to results of computer simulations. We use the same material parameters in the model and in the simulation and are thus able to conclude about the quality of the model. We ran six simulations in which we changed the impact velocity (1.5 and 2.5 Km/s), the slope of the strength-pressure relation (0.5 and 1), and the cap pressure (10 and 4 GPa). In reference 1 we expressed the dynamic pressure as $\frac{1}{2} \rho_t u^2$. But the pressure decreases radially. To compensate for this decrease, and also to get a measure for the extent of disagreement between model and simulation, we reran the model with the dynamic pressure replaced by $\frac{1}{2} k\rho_t u^2$ ($k \leq 1$).

By comparing model predictions to simulation results we draw the following conclusions:

1. At 1.5 Km/s, the original model (K = 1) predicts R_t to within 5%. This validates that the model represents the essential physical processes occuring in the simulation.
2. The model represents reasonably well the increase of R_t with the slopes (α_1, α_2), the increase of R_t with the cap pressure (P_1, P_2), and the increase of R_t with impact velocity (V).
3. Comparing the model prediction to the true resistance (R_t) we get best agreement with k = 0.8 to 0.9 for 1.5 Km/s and $k \cong 0.6$ for 2.5 Km/s. This decrease of k with velocity may be due to a radial flow field effect, or to the localization of the flow field, which is relatively faster at higher velocities. We hope to clarify this in the future.

References

[1] Y. Partom, "Ceramic armor resistance to Long Rod Penetration (R_t) and Its Dependence on Projectile Velocity," IAT.R 0017, March 1993.

[2] A. Tate, "Theory for the Deceleration of Long Rods after Impact," J. Mech. Phys. Solids, 15, 38 (1967).

[3] R. F. Bishop, R. Hill and N. F. Mott, "The Theory of Indentation and Hardness Tests," Proc. Phys. Soc., 57, 148 (1945).

[4] J. M. McGlaun, S. L. Thompson and M. G. Elrick, "CTH: A Three Dimensional Shock Wave Physics Code," Int. J. Impact Engng., 10, 351 (1990).

[5] C. E. Anderson, et al., "Target Resistance for Long Rod Penetration into Semi-Infinite Targets," Impact III Seminar, Univ. of Tokyo, Aug. 1991.

Distribution List

Administrator
Defense Technical Information Center
Attn: DTIC-DDA
8725 John J. Kingman Road, Ste 0944
Ft. Belvoir, VA 22060-6218

Director
US Army Research Lab
ATTN: AMSRL OP SD TA
2800 Powder Mill Road
Adelphi, MD 20783-1145

Director
US Army Research Lab
ATTN: AMSRL OP SD TL
2800 Powder Mill Road
Adelphi, MD 20783-1145

Director
US Army Research Lab
ATTN: AMSRL OP SD TP
2800 Powder Mill Road
Adelphi, MD 20783-1145

Director
US Army Research Lab
ATTN: AMSRL OP AP L (305)
APG MD 21005-5066

Director
Army Research Laboratory
AMSRL-CI-LP
Technical Library 305
APG, MD 21005-5066